JOURNAL OF BACTERIOLOGY, Sept. 1998, p. 4466–4474 Vol. 180, No. 17
0021-9193/98/$04.00+0

Similarities between the *antABC*-Encoded Anthranilate Dioxygenase and the *benABC*-Encoded Benzoate Dioxygenase of *Acinetobacter* sp. Strain ADP1

BECKY M. BUNDY, ALAN L. CAMPBELL, AND ELLEN L. NEIDLE*

Department of Microbiology, University of Georgia, Athens, Georgia 30602-2605

Received 4 May 1998/Accepted 18 June 1998

***Acinetobacter* sp. strain ADP1 can use benzoate or anthranilate as a sole carbon source. These structurally similar compounds are independently converted to catechol, allowing further degradation to proceed via the β-ketoadipate pathway. In this study, the first step in anthranilate catabolism was characterized. A mutant unable to grow on anthranilate, ACN26, was selected. The sequence of a wild-type DNA fragment that restored growth revealed the *antABC* genes, encoding 54-, 19-, and 39-kDa proteins, respectively. The deduced AntABC sequences were homologous to those of class IB multicomponent aromatic ring-dihydroxylating enzymes, including the dioxygenase that initiates benzoate catabolism. Expression of *antABC* in *Escherichia coli*, a bacterium that normally does not degrade anthranilate, enabled the conversion of anthranilate to catechol. Unlike benzoate dioxygenase (BenABC), anthranilate dioxygenase (AntABC) catalyzed catechol formation without requiring a dehydrogenase. In *Acinetobacter* mutants, *benC* substituted for *antC* during growth on anthranilate, suggesting relatively broad substrate specificity of the BenC reductase, which transfers electrons from NADH to the terminal oxygenase. In contrast, the *benAB* genes did not substitute for *antAB*. An *antA* point mutation in ACN26 prevented anthranilate degradation, and this mutation was independent of a *mucK* mutation in the same strain that prevented exogenous muconate degradation. Anthranilate induced expression of *antA*, although no associated transcriptional regulators were identified. Disruption of three open reading frames in the immediate vicinity of *antABC* did not prevent the use of anthranilate as a sole carbon source. The *antABC* genes were mapped on the ADP1 chromosome and were not linked to the two known supraoperonic gene clusters involved in aromatic compound degradation.**

Both the role of anthranilate as an intermediary metabolite in tryptophan degradation and the existence of bacteria able to use anthranilate as a sole source of carbon and energy have been known for many years (22). Nevertheless, the first step in the aerobic degradation of anthranilate by bacteria remains poorly characterized. Early attempts to purify the multicomponent enzyme responsible for the initial oxidation step proved to be unsuccessful. These attempts did, however, establish that anthranilate was oxidized when two distinct *Pseudomonas* protein fractions and Fe^{2+} were present (26). Catechol was identified as the product of anthranilate dihydroxylation, and the corresponding enzyme was shown to be a di- rather than a mono-oxygenase (27, 46). No further information about this anthranilate 1,2-dioxygenase (deaminating, decarboxylating; EC 1.14.12.1) has been reported in nearly 30 years.

Recently there has been renewed interest in microbial dioxygenases (4, 6). This interest has stemmed in part from their importance in degrading a vast array of aromatic compounds in the environment, in part from a fundamental concern about their biochemistry, and in part from their potential use in bioremediation. Compounds similar in structure to anthranilate, such as benzoate (Fig. 1) or 2-chlorobenzoate, are substrates of multicomponent ring-hydroxylating dioxygenase systems (13, 18, 34). Several classes of these dioxygenases have been defined based on the number of components, the types of iron-sulfur clusters involved, and the types of flavin cofactors (4, 6). The chromosomal *benABC* genes of the soil bacterium *Acinetobacter* sp. strain ADP1 encode a class IB dioxygenase that converts benzoate to a nonaromatic diol. Further catabolism of this diol yields catechol, which is also the product of anthranilate oxidation. The pathways for anthranilate and benzoate degradation by strain ADP1, therefore, are convergent (Fig. 1). By using a strategy based on previous studies of benzoate and catechol degradation by ADP1 (14, 47), it was possible to select mutants unable to convert anthranilate to catechol.

In this report, the characterization of one such ADP1-derived anthranilate dioxygenase mutant is described. The natural transformability of the *Acinetobacter* strains used in these studies facilitated the identification of the wild-type *antABC* genes, which restored growth of the mutant with anthranilate as the sole carbon source. These *ant* genes, shown to encode anthranilate dioxygenase, were homologous in sequence to the benzoate dioxygenase-encoding *benABC* genes. Comparisons between the regulation and functions of the *antABC* genes and those of their better-studied *ben* counterparts were made. Whereas the formation of catechol from anthranilate required only the dioxygenase-catalyzed step, catechol formation from benzoate requires a second enzymatic step that is catalyzed by the *benD*-encoded dehydrogenase (Fig. 1) (33). Studies of the similar, but distinct, *ant*- and *ben*-encoded multicomponent dioxygenases may reveal key features of enzyme substrate specificity and catalytic efficiency.

* Corresponding author. Mailing address: Department of Microbiology, University of Georgia, 527 Biological Sciences Building, Athens, GA 30602-2605. Phone: (706) 542-2852. Fax: (706) 542-2674. E-mail: eneidle@arches.uga.edu.

MATERIALS AND METHODS

Bacterial strains and growth conditions. *Acinetobacter* strains are listed in Table 1. *Acinetobacter* strains were derived from BD413, also designated ADP1 (24). Taxonomic confusion has led to the *Acinetobacter calcoaceticus* species designation for ADP1 being discontinued until further characterization is com-

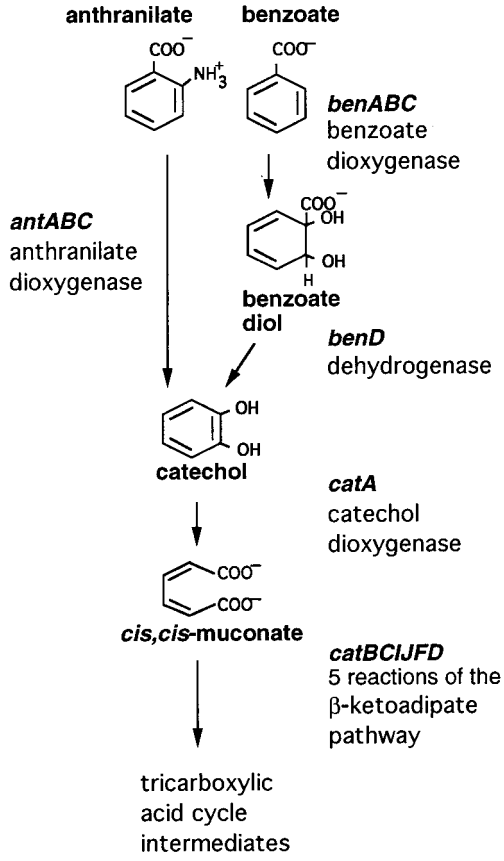

FIG. 1. Degradation of anthranilate and benzoate via the β-ketoadipate pathway. Relevant compounds, genes, and enzymes are indicated.

plete (11a). *Escherichia coli* DH5α (Gibco BRL), S17-1 (43), and BL21(DE3) (44) were used as plasmid hosts. Bacteria were cultured in Luria-Bertani broth and minimal medium at 37°C as previously described (39, 42). Carbon sources were added to minimal medium at the following final concentrations: 10 mM succinate, 3 mM benzoate, 3 mM 4-hydroxybenzoate, 3 mM *cis,cis*-muconate, 2.5 mM anthranilate, or 2 mM catechol. Antibiotics were added as needed at the following final concentrations: tetracycline, 6 μg/ml; kanamycin, 20 μg/ml; streptomycin, 25 μg/ml; spectinomycin, 25 μg/ml; and ampicillin, 150 μg/ml for *Acinetobacter* strains and 80 μg/ml for *E. coli*.

DNA manipulation and plasmid construction. Standard methods were used for all chromosomal and plasmid DNA purifications, restriction enzyme digestions, electrophoreses, ligations, and *E. coli* transformations (39). Plasmids are described in Table 1 and Fig. 2. To isolate a chromosomal ADP1 DNA fragment carrying the *ant* genes, a recombinant plasmid library was constructed. Chromosomal ADP1 DNA was digested with *Hin*dIII. Following electrophoretic separation, fragments of various size ranges were purified from a 0.7% agarose gel with the GeneClean purification kit (Bio101). A fraction of DNA in the 4- to 6-kbp size range was ligated to the cloning vector pZero2.1 (Invitrogen) and used to transform *E. coli* DH5α. This vector enables transformants with recombinant plasmids to be selected on medium with kanamycin. Plasmid pBAC103 (Fig. 2) was one of the recombinant plasmids generated. Subclones of pBAC103 and pBAC163, whose isolation is described below, were constructed by standard methods (39).

To disrupt plasmid-borne genes, omega cassettes that can be excised from pUI1637 or pUI1638 with one of several restriction endonucleases were used. The cassette from pUI1638 (ΩS) confers resistance to spectinomycin and streptomycin (12, 37). That from pUI1637 (ΩK) confers resistance to kanamycin (12). Transcriptional and translational stop signals follow each drug resistance determinant. In two plasmids, pBAC143 and pBAC112, *antC* was disrupted by ΩS (Table 1). In pBAC156, the *benC* gene was disrupted by ΩK (Table 1). Open reading frames (ORFs) near the *ant* genes were disrupted on plasmids pBAC141 (ORF2::ΩS), pBAC176 (ORF1::ΩK), and pBAC244 (ORF3::ΩS) (Table 1). Plasmid pBAC162 was constructed to generate strains with chromosomal *antA*::*lacZ* transcriptional fusions (Table 1). A promoterless *lacZ* cartridge that also confers Km^r was used (28). Plasmids pBAC214, pBAC226, pBAC241, and pBAC147 (Table 1) were used to determine the mutation in the *antA5024* allele as described below.

***Acinetobacter* transformation, strain construction, and chromosomal mapping.** Naturally competent *Acinetobacter* strains were transformed by linear

TABLE 1. Bacterial strains and plasmids

Strain or plasmid	Relevant characteristic(s)	Reference or source
Acinetobacter strains		
ADP1	Wild type (BD413)	24
ADP205	Δ(*catM-catB3205*)	32
ACN24	Δ(*catM-catB3205*) *antA5024 mucK5024*	This study
ACN26	*antA5024 mucK5024*	This study
ACN30	*trpD1*::Ω*S*	16
ACN80	Δ(*antC-orf3*)::Ω*S5080*	This study
ACN84	*antA5024*	This study
ACN86	*antC*::ΩS5086	This study
ACN87	Δ(*benB-benC5129*) *antC*::ΩS5086	This study
ACN88	*orf2*::Ω*S5088* Δ(*antA-orf3 5088*)	This study
ACN103	*benM*::Ω*K5008 antC*::Ω*S5086*	This study
ACN106	*benC*::Ω*K5106*	This study
ACN107	*antA*::*lacZ*-Km^r *5107*	This study
ACN115	*benC*::Ω*K5106 antC*::Ω*S5086*	This study
ACN120	*orf2*::Ω*S5088 antA*::*lacZ*-Km^r *5107*	This study
ACN129	Δ(*benB-benC5129*)	9
ACN130	*orf1*::Ω*K5130*	This study
ACN191	*orf3*::Ω*S5191*	This study
ACN194	*orf3*::Ω*S5191 antA*::*lacZ*-Km^r *5107*	This study
ACN204	*orf2*::Ω*S5088*	This study
ISA25	Δ(*catB-catF4025*)	14
Plasmids[a]		
pADPW4	Wild-type *mucK*	47
pCyt3	Ap^r Tc^r expression vector	3
pIB1	Wild-type *catBCIJFD*	31
pKOK6	Source of promoterless *lacZ*-Km^r cassette	28
pRK415	Tc^r broad host range cloning vector	25
pT7-7	Ap^r expression vector	45
pUC19	Ap^r cloning vector	49
pUI1637	Source of ΩK	12
pUI1638	Source of ΩS	12
pWH845	Ap^r expression vector for *Acinetobacter*	40
pZero2.1	Km^r cloning vector	Invitrogen
pBAC105	Deletion of DNA between *Cla*I sites in *antA* and ORF3 of pBAC103 (Fig. 2)	This study
pBAC112	ΩS(*Bam*HI[b]) replacement of *Bgl*II fragment in pBAC103 (*antC* to ORF3 [Fig. 2])	This study
pBAC141	ΩS(*Eco*RV[b]) in ORF2 *Ssp*I site (Fig. 2) of pBAC105	This study
pBAC143	ΩS(*Eco*RV[b]) in *antC Ssp*I site of pBAC132 (Fig. 2)	This study
pBAC146	*Hin*dIII-*Sal*I fragment of pBAC103 (from ORF2 through *antC* [Fig. 2]) in pCyt3	This study
pBAC147	PCR-amplified DNA of *antA5024* allele between *Cla*I and *Nsi*I sites (Fig. 2) in pUC19	This study
pBAC156	ΩK(*Cla*I[b]) in *benC Cla*I site (5303[c]) of *ben* gene fragment (4764 to 7874[c]) in pUC19 vector	This study
pBAC162	*lacZ*-Km^r (*Pst*I[d]) in *antA Nsi*I site of pBAC109 (Fig. 2)	This study
pBAC176	ΩK(*Eco*RV[b]) in ORF1 *Eco*RV site of pBAC163 (Fig. 2)	This study
pBAC189	*antABC Swa*I (2007[e])-*Hin*dIII (6524[e]) DNA in pWH845	This study
pBAC190	*antABC Swa*I (2007[e])-*Hin*dIII (6524[e]) DNA in pT7-7	This study
pBAC194	*lacZ*-Km^r (*Bam*HI[d]) in *antC Bgl*II site (Fig. 2) of pBAC146	This study
pBAC214	Deletion of between *Cla*I sites in *antA* and *antB* of pBAC146 (Fig. 2)	This study
pBAC226	ADP1 DNA insert of pBAC214 cloned in pRK415	This study
pBAC241	*antA5024* isolated by gap repair using pBAC226	This study
pBAC244	ΩS(*Bam*HI[b]) in ORF3 *Bgl*II site of pBAC145 (Fig. 2)	This study

[a] Additional plasmids are shown in Fig. 2.
[b] Restriction endonuclease used to excise Ω cassette from pUI1637 or pUI1638.
[c] Position in the *ben-cat* sequence under GenBank accession no. AF009224.
[d] Restriction endonuclease used to excise *lacZ*-Km^r cassette from pKOK6.
[e] Position in the *antABC* sequence of GenBank accession no. AF071556.

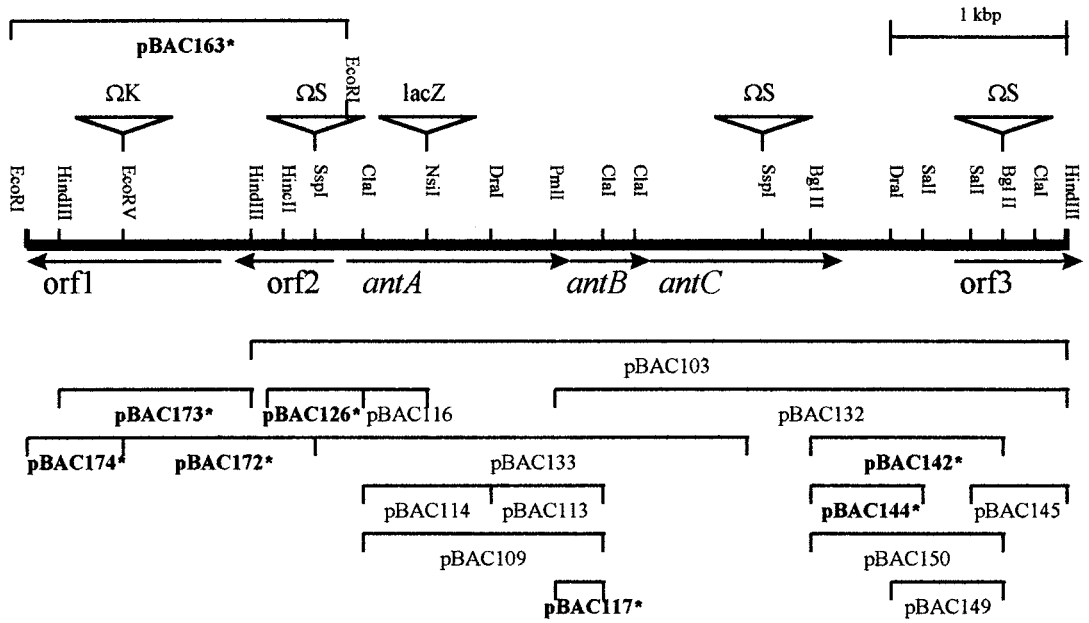

FIG. 2. Restriction map of the 6.5-kbp chromosomal *antABC* region. The locations of genes, and their transcriptional directions, are shown relative to some of the restriction endonuclease recognition sites. Lines indicate the DNA regions contained on recombinant pBAC plasmids. Plasmids shown in boldface and marked by an asterisk were constructed with the pUC19 vector, and all others were constructed with the pZero2.1 vector. The insertion sites of either omega or *lacZ* cassettes correspond to those in strains and plasmids described in Table 1.

DNA, plasmid DNA, or crude DNA lysates as previously described (16, 23, 32). Some plasmids were introduced into *Acinetobacter* recipients by conjugation from *E. coli* S17-1 (32, 43). Plasmids carrying modified regions of ADP1 DNA on replicons that are not stably maintained in *Acinetobacter* were used to transform recipients, yielding new strains in which homologous recombination had replaced the wild-type chromosomal allele with the modified version. Strains ACN80 and ACN86 were constructed by this method with the *antC*-disrupted plasmids pBAC112 and pBAC143, respectively. The latter plasmid was used to generate ACN87 with ACN129 as the recipient strain. ACN103 was constructed by similar methods with chromosomal disruptions of both *antC* and *benM* (8). Strains constructed with ADP1 as the recipient include ACN88 (by using pBAC141), ACN106 (by using pBAC156), ACN107 (by using pBAC162), ACN130 (by using pBAC176), ACN169 (by using pBAC194), and ACN204 (by using pBAC141). Strain ACN194 was generated by using ACN107 as the recipient and pBAC244 as the donor DNA. This plasmid was also the source of the disrupted ORF3 allele in ACN191. Southern hybridization analyses confirmed that the mutated plasmid alleles replaced the corresponding wild-type regions of the chromosome without integration of the entire plasmid.

In some cases, a mutation in one *Acinetobacter* strain was incorporated into the chromosome of a second strain by making a crude DNA lysate of the first strain and using it to transform the second strain (16, 23). With this method, ACN115 was generated from ACN86 and ACN106, ACN118 was generated from ACN107 and ISA29, ACN119 was generated from ACN107 and ISA25, ACN120 was generated from ACN107 and ACN88, and ACN170 was generated from ACN169 and ACN88. In the latter two strains, the *antA*::*lacZ* fusion of the donor replaced the deleted *antABC* region of the recipient. Southern hybridizations confirmed the expected chromosomal configurations.

To determine the locations of the *antABC* genes on the ADP1 chromosome, intact genomic DNA was prepared and digested as previously described (16). The conditions for transverse alternating-field electrophoresis were the same as those of previous studies (16).

Isolation of chromosomal DNA in the region upstream of *antA*. In ACN88, the ΩS chromosomal insertion lies in ORF2 and introduces an *Eco*RI recognition site not present in the wild-type strain (Table 1 and Fig. 2). Chromosomal DNA from ACN88 was digested with *Eco*RI and ligated to *Eco*RI-digested DNA of the cloning vector pUC19. Following transformation of an *E. coli* host with the ligated DNA, a single transformant with resistance to streptomycin and spectinomycin, characteristic of the ORF2::ΩS allele, was obtained. This transformant harbored plasmid pBAC163 (Fig. 2), and subsequent Southern hybridization and DNA sequence analyses confirmed that pBAC163 carries DNA from the chromosomal region upstream of *antA*.

Southern hybridization and DNA sequence analyses. Southern hybridization analyses were performed as previously described (16). DNA probes were labeled with digoxigenin by random priming, and probes were detected with antidigoxigenin-alkaline phosphatase conjugates and chemiluminescent substrates according to the Genius System instructions (Boehringer Mannheim Corp.).

The DNA sequences of plasmids pBAC103 and pBAC163 and their subclones (Fig. 2) were determined with double-stranded templates and sequencing primers, purchased from Promega, that recognize the cloning vector. In addition, 15 oligonucleotides, purchased from Genosys Biotechnologies Inc., were used as primers in sequencing reactions (Table 2). In these reactions, oligonucleotides 1 to 4 were used with pBAC163 as the template DNA. The other oligonucleotides were used with pBAC103. An automated DNA sequencer (ABI373A; Applied Biosystems, Inc.) was used in the University of Georgia Molecular Genetics Instrumentation Facility. DNA sequences were analyzed with the Wisconsin Genetics Computer Group programs (11).

Determination of the sequence of the mutation in the *antA5024* allele. Two different approaches were used to identify the mutation(s) causing the temperature-sensitive defect in AntA. In the first approach, the mutant allele was amplified from purified chromosomal DNA by using oligonucleotides 5 and 10 (Table 2) as primers in a PCR with *Pfu* DNA polymerase according to the instructions of the polymerase supplier (Stratagene). Dimethyl sulfoxide was added to com-

TABLE 2. Oligonucleotides used in DNA sequencing reactions

Designation	Approximate location	Nucleotide position[a]
1	ORF1	232–252
2	ORF1	683–703
3	ORF1	1288–1308
4[b]	ORF2	1638–1657
5	*antA*	2191–2211
6[b]	*antA*	2272–2292
7	*antA*	2493–2513
8[b]	*antA*	2572–2592
9	*antA*	2572–2592
10[b]	*antA*	3328–3348
11	*antB*	3663–3683
12	*antB*	4071–4091
13[b]	*antC*	4117–4137
14	*antC*	4529–4549
15[b]	*antC*	5108–5128

[a] Positions correspond to those of the 6,529-bp *ant* region sequence (GenBank accession no. AF071556) and indicate the DNA sequences (5′-3′) of oligonucleotides 1, 2, 3, 5, 7, 9, 11, 12, and 14.

[b] The sequence is that of the reverse complement of the nucleotide positions indicated.

prise 10% of the total reaction volume. The PCR-amplified DNA product was gel purified by using the QIAquick Gel Extraction kit (Qiagen) and digested with *Cla*I and *Nsi*I. This DNA was ligated to the cloning vector pUC19 (49), which had been digested with *Acc*I and *Pst*I to form pBAC147. The sequence of *Acinetobacter* DNA of pBAC147 was determined with primers (from Promega) that recognized the pUC19 vector as described above.

In the second approach, gap repair methods (17) were used to isolate chromosomal DNA in the *antA* region of ACN84. With this technique, a recipient strain is transformed with a linearized plasmid such that homologous recombination between plasmid and chromosomal DNA segments generates a circularized plasmid in vivo. The transforming plasmid is linearized to create a gap between two regions of homology, forcing recombination to occur upstream and downstream of the desired chromosomal region, in this case the mutant *antA* DNA. The recombinant plasmid generated in vivo therefore will carry the appropriate chromosomal DNA segment (17). Plasmid pBAC226 was digested with *Cla*I to yield a linear fragment, and this DNA was used to transform ACN84. Homologous recombination in vivo between plasmid and chromosomal DNA sequences yielded a circular plasmid, pBAC241, carrying the *antA5024* allele. The appropriate oligonucleotides (Table 2) were used for DNA sequence determinations.

AntABC and β-galactosidase assays. To measure anthranilate dioxygenase activity, cell extracts were prepared by sonication as previously described for other enzymes of the β-ketoadipate pathway (42). Anthranilate dioxygenase was assayed spectrophotometrically by monitoring the decrease in anthranilate concentration as indicated by A_{310} (26). Protein concentrations were determined by the method of Bradford (5), using bovine serum albumin as the standard.

For β-galactosidase assays, *Acinetobacter* cultures were grown overnight in 5 ml of Luria-Bertani broth with or without the addition of inducers, 3 mM benzoate, 3 mM *cis,cis*-muconate, 2.5 mM anthranilate, or 2 mM catechol. Cells were lysed with chloroform and sodium dodecyl sulfate. Following the removal of cell debris by centrifugation, the β-galactosidase activity in the supernatant fraction was determined as described by Miller (29).

Metabolite monitoring by HPLC. For metabolite monitoring, *E. coli* cultures (10 ml) were grown overnight on M9 medium with glucose as a carbon source (39). *Acinetobacter* cultures were similarly grown on minimal medium with either 10 mM succinate or 4 mM anthranilate as the carbon source. Since ADP1 (pBAC189) was unable to use anthranilate as the sole carbon source, it was grown with both 10 mM succinate and 2 mM anthranilate. When appropriate, ampicillin was added for plasmid maintenance. Cultures were diluted with 15 ml of the minimal medium used for overnight growth, and in some cases, 250 μM isopropyl-β-D-thiogalactopyranoside (IPTG) was added to induce gene expression from the vector's *lac* promoter. Monitoring was initiated after the addition of approximately 1 mM anthranilate.

To monitor anthranilate metabolism, 1-ml culture samples were centrifuged to pellet cells. Any cells remaining in the supernatant fractions were removed by passage through a low-protein-binding, 0.22-μm-pore-size syringe filter (MSI). A 20-μl sample of the filtrate was analyzed on a C_{18} reversed-phase high-performance liquid chromatography (HPLC) column from Bio-Rad Laboratories. Elution at a rate of 0.8 ml/min was carried out with 30% acetonitrile and 0.1% phosphoric acid, and the eluant was monitored by UV detection at 282 nm. Under these conditions, the retention times for anthranilate, catechol, and *cis,cis*-muconate were 6.0, 4.6, and 3.2 min, respectively. Peak areas corresponding to standards and experimental samples were calculated by using the Valu-Chrom software package from Bio-Rad Laboratories.

Nucleotide sequence accession number. The sequence of the 6,529-bp *antABC* region was deposited in the GenBank database (accession no. AF071556).

RESULTS

Isolation of a mutant, ACN26, unable to degrade anthranilate. The endogenous accumulation of *cis,cis*-muconate (Fig. 1) is toxic (14). Therefore, the presence of a compound that can be converted to this metabolite prevents growth of strains in which the subsequent metabolism of *cis,cis*-muconate is blocked, even when an additional carbon source is available (14). Selection for growth under these conditions can yield mutants that are unable to form *cis,cis*-muconate. For example, the presence of benzoate in the growth media of *catB* deletion strains has selected mutants that do not convert benzoate to *cis,cis*-muconate (47). It seemed likely, therefore, that a similar strategy could be used to isolate spontaneous mutants unable to catalyze the initial hydroxylation of anthranilate. Strain ADP205 (Table 1), which cannot degrade *cis,cis*-muconate because of a *catMBC* deletion, was grown on solid medium with 3 mM 4-hydroxybenzoate as the carbon source in the presence of 1 mM anthranilate, the potential source of the toxic intermediate. Mutations preventing the conversion of anthranilate to catechol, or those preventing the conversion of catechol to *cis,cis*-muconate, should allow growth. Whereas mutations of the first type were of interest, mutations of the second type predominated as indicated by catechol production (data not shown).

To identify the desired mutants, anthranilate-tolerant strains were individually transformed by the *catMBC* genes that were provided as linear DNA from *Xba*I-digested plasmid pIB1 (Table 1). Previously described methods were used (31, 32), and transformants were selected with benzoate as the sole carbon source to ensure repair of the chromosomal deletion. Under these conditions, anthranilate dioxygenase mutants, but not catechol dioxygenase mutants, should grow, since catechol dioxygenase is needed to degrade benzoate (Fig. 1). Only one transformant that could grow on benzoate was obtained, ACN26 (derived from the *catM-catB* deletion parent ACN24). This strain was unable to use either anthranilate or *cis,cis*-muconate as the sole carbon source at 39°C. ACN26 could, however, use anthranilate as the sole carbon source at 25°C.

Different mutations affect *cis,cis*-muconate and anthranilate metabolism. ACN26 can degrade endogenous *cis,cis*-muconate since it grows on benzoate. Mutations in the *mucK* gene, encoding a transport protein, are known to prevent growth on exogenous *cis,cis*-muconate (47). Therefore, the effect of introducing a wild-type *mucK* gene into ACN26 was tested. ACN26 was transformed with DNA from plasmid pADPW4, carrying *mucK*, and a resultant strain was designated ACN84. ACN84 grew with *cis,cis*-muconate as the sole carbon source, indicating that ACN26 carries a defective *mucK* gene. ACN84 remained unable to grow on anthranilate as the sole carbon source at 39°C. It is not clear why a mutation in *mucK* was isolated in the selection for a strain unable to convert anthranilate to *cis,cis*-muconate. Since similar selections led to the isolation of strains with mutations in both *mucK* and the structural genes encoding biodegradative enzymes (47), it may be that *cis,cis*-muconate exported from adjacent cells under these isolation conditions contributes to selective pressure for loss of the MucK uptake activity.

Isolation of the *ant* genes. A fraction of 4- to 6-kbp *Hin*dIII-digested ADP1 DNA was able to transform ACN26 to grow on anthranilate. Following ligation to a vector, this DNA was introduced into *E. coli* as described in Materials and Methods. The recombinant plasmid-bearing colonies were patched individually to solid anthranilate medium onto which ACN26 cells had been spread. *E. coli*, which does not use anthranilate as a carbon source, can donate plasmid DNA in the natural transformation of ACN26. Plasmid DNA able to repair the ACN26 mutation should allow growth. The recombinant plasmids were not used in *trans* to complement ACN26 directly, because the cloning vector is not stably maintained in *Acinetobacter*, thereby making it difficult to retrieve DNA that restored growth by homologous recombination. Of several hundred *E. coli* colonies screened, one carried a plasmid, pBAC103, that restored growth of ACN26 on anthranilate. This plasmid, with 4.9 kbp of ADP1 DNA, and subclones derived from it were used for DNA sequence determination (Fig. 2) (see Materials and Methods). Sequence analyses revealed several ORFs (Fig. 2), three of which were designated *antABC* based on their homology to a number of dioxygenase-encoding genes, described below.

Homology between AntABC and aromatic ring-hydroxylating dioxygenases. By database searches with the deduced amino acid sequences, the 54-kDa AntA and 19-kDa AntB were found to be homologs of the large and small subunits, respectively, of the terminal oxygenases of class IB dioxygenases. The 39-kDa AntC resembled the reductase components associated with these oxygenases. In pairwise alignments of the Ant proteins with their counterparts, the percentage of identical aligned residues ranged from 33 to 46% (Tables 3 to 5). En-

TABLE 3. Similarity between large subunits of the terminal dioxygenases

Protein	% Similarity (identity) with:				
	AntA	XylX	BenA	CbdA	TftA
AntA	100 (100)	67 (46)	65 (44)	64 (43)	59 (40)
XylX		100 (100)	77 (63)	78 (55)	60 (40)
BenA			100 (100)	70 (55)	57 (36)
CbdA				100 (100)	57 (37)
TftA					100 (100)

TABLE 4. Similarity between small subunits of the terminal dioxygenases

Protein	% Similarity (identity) with:				
	AntB	XylY	BenB	CbdB	TftB
AntB	100 (100)	57 (36)	59 (37)	58 (39)	57 (33)
XylY		100 (100)	77 (61)	73 (57)	57 (35)
BenB			100 (100)	70 (53)	55 (35)
CbdB				100 (100)	53 (33)
TftB					100 (100)

zymes most similar to AntABC included the highly specific benzoate dioxygenase and a toluate dioxygenase, with broad specificity, that dihydroxylates both benzoate and substituted benzoates. The former is encoded by the ADP1 chromosomal *benABC* genes, and the latter is encoded by the *Pseudomonas putida xylXYZ* genes of the TOL plasmid pWW0 (19, 34). Also homologous to *antABC* were the *cbdABC* genes, isolated from a conjugative plasmid of *Burkholderia cepacia* (18). The CbdABC proteins catalyze the dihydroxylation of 2-halobenzoates, yielding catechol. Additional homologs of *antA* and *antB* included the *B. cepacia tftA* and *tftB* genes, which encode the large and small subunits of a 2,4,5-trichlorophenoxyacetic acid terminal oxygenase (10). The proposed roles of AntABC are analogous to those of BenABC (Fig. 3).

Identification of the mutation that prevents growth on anthranilate. Plasmid pBAC116 (Fig. 2) transformed ACN26 and ACN84 to grow with anthranilate at 39°C, thereby localizing their mutations to a 298-bp region between the *Cla*I and *Nsi*I restriction recognition sites of the *antA* gene. The corresponding region of ACN84 was isolated by gap repair methods (17), and DNA sequence determination revealed a point mutation in the 43rd codon of the *antA* structural gene that changed a T to an A (position 2307 in the sequence under GenBank accession no. AF071556). This same mutation was identified independently by PCR amplification of the chromosomal region with *Pfu* DNA polymerase (see Materials and Methods). As illustrated in Fig. 4, this mutation should cause a conserved methionine residue to be replaced by a lysine in the N-terminal region of the mutant protein.

The *antABC* genes enable catechol to be formed from anthranilate. In *E. coli*, expression of the *antABC* genes, on plasmid pBAC190 (Table 1), allowed 1 mM anthranilate to be converted to catechol in approximately 4 h (Fig. 5A). A diol intermediate was not detected by the HPLC monitoring techniques. An isogenic strain carrying only the cloning vector did not metabolize anthranilate under identical conditions (data not shown).

Surprisingly, the *antABC* genes in *trans* on pBAC189 (Table 1) did not complement the inability of either ACN26 or ACN84 to use anthranilate as a sole carbon source. In addition, pBAC189 suppressed the ability of the wild-type *Acinetobacter* strain ADP1 to use anthranilate as the sole carbon source. ADP1(pBAC189) grew, however, when succinate was provided together with anthranilate. It is possible that succinate allows growth by reducing expression of the *antABC* genes compared to that when only anthranilate is available as the carbon source. Consistent with this possibility, ADP1(pBAC189) that was grown with both compounds and then provided with 1 mM anthranilate removed all detectable anthranilate from the medium in approximately 4 h, a rate slightly lower than that of ADP1 that had been grown on anthranilate (Fig. 5B).

During the initial phase of anthranilate catabolism by ADP1 (pBAC189), a small amount of catechol was detected, approximately 30 μM at 1.5 h after anthranilate addition (Fig. 5B, bottom). In contrast, no catechol was detected during anthranilate catabolism by ADP1 that had initially been grown with either anthranilate (Fig. 5B, bottom) or succinate (data not shown). *cis,cis*-Muconate was detected during anthranilate catabolism by ADP1 and ADP1(pBAC189) (Fig. 5B, bottom). Since expression of the *antABC* genes in *trans* in *Acinetobacter* led to the formation of a higher-than-normal level of catechol during anthranilate catabolism, catechol may contribute to the inhibition of growth by ADP1(pBAC189) with anthranilate as the sole carbon source.

Anthranilate-mediated induction. Anthranilate-grown ADP1 consumed anthranilate immediately upon its addition to the culture, whereas with succinate-grown cells there was a delay of approximately 2 h before consumption was detected (data not shown). It appeared that the anthranilate degradation pathway, like similar pathways, was inducible. Consistent with this, anthranilate dioxygenase activity in cell extracts of anthranilate-grown wild-type cells was approximately 0.03 μmol per min per mg of protein. In succinate-grown cells, the activity was undetectable (less than 0.005 μmol per min per mg of protein).

To characterize transcriptional-level regulation, strain ACN107, in which the chromosomal *antA* gene was replaced with an *antA*::*lacZ* transcriptional fusion (Fig. 2), was constructed. β-Galactosidase (LacZ) activity was measured in stationary-phase cultures. The presence of anthranilate in the growth medium of ACN107 increased LacZ levels to 16,814 ± 2,337 Miller units, compared to 76 ± 47 Miller units in the absence of added inducers. To ensure that induction resulted from anthranilate itself and not a subsequent metabolite, HPLC monitoring was used to confirm that there was no detectable catabolism of anthranilate by the *antA*-disrupted ACN107 (data not shown). Neither catechol nor *cis,cis*-muconate significantly increased expression of the *antA*::*lacZ* fusion relative to that in uninduced cultures (data not shown).

Three ORFs near *antABC* are not required for anthranilate degradation. Since genes encoding transcriptional activators are often adjacent to the targets of their regulation, the DNA upstream of *antA* was isolated on pBAC163 as described in Materials and Methods. The small, 417-bp ORF2 (Fig. 2) immediately upstream of *antA* was disrupted on the chromosome

TABLE 5. Similarity between reductase components

Protein	% Similarity (identity) with:			
	AntC	XylZ	BenC	CbdC
AntC	100 (100)	60 (43)	61 (38)	62 (40)
XylZ		100 (100)	71 (53)	65 (48)
BenC			100 (100)	68 (51)
CbdC				100 (100)

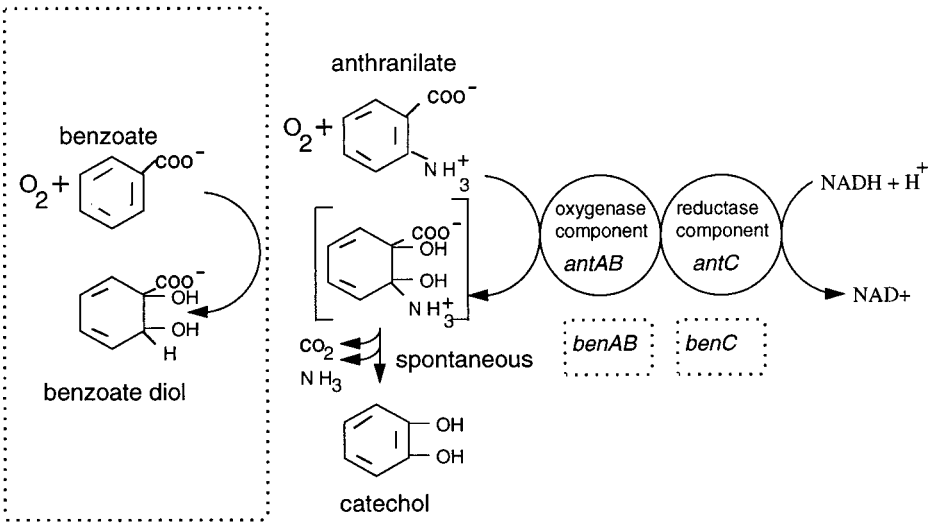

FIG. 3. Proposed functions of the *ant* gene-encoded proteins. By comparison with the functions of the *ben* gene-encoded benzoate dioxygenase, indicated in the boxes, the *antAB* genes encode the terminal dioxygenase and *benC* encodes the reductase of a class IB dihydroxylating multicomponent dioxygenase.

of the wild-type strain and that of a strain with the *antA*::*lacZ* fusion to generate strains ACN204 and ACN120, respectively. Strain ACN204 was able to use anthranilate as the sole carbon source. Moreover, the ORF2 disruption of ACN120 did not alter the ability of anthranilate to induce expression of the *lacZ* fusion. The presence of anthranilate in the growth medium of ACN120 increased LacZ levels to 15,494 ± 1,781 Miller units, compared to 64 ± 37 Miller units in the absence of added inducers. ORF2, therefore, did not appear to regulate transcription of the *antABC* genes. In addition, disruption of ORF2 did not have a *cis*-acting effect on transcriptional regulation.

ORF2 was not similar to sequences in the databases, whereas homologs to ORF1 and ORF3, near *antABC* (Fig. 2), were detected. Although the complete sequence of ORF1 has not been determined, its 5′ region was homologous to those encoding dehydrogenases of a related family that includes PdxB, an enzyme that oxidizes 4-phosphoerythronate in the biosynthetic pathway for pyridoxine (vitamin B_6) (41). In an alignment of 147 amino acids of PdxB with the ORF1-encoded peptide sequence, 47% of the residues were identical. Disruption of ORF1 on the chromosome of strain ACN130 (Table 1) did not prevent the use of anthranilate as a sole carbon source.

The 5′ region of ORF3, whose complete sequence has not been determined, resembled genes in a family encoding AraC/XylS-type transcriptional activators (15). One member of this family, a putative regulatory protein of *P. putida*, was 40% identical to the ORF3-encoded peptide in a 76-amino-acid region (37a). In ACN191 the chromosomal copy of ORF3 was disrupted (Table 1), and, like ACN130, ACN191 remained capable of growth with anthranilate as the sole carbon source. In addition, expression of the chromosomal *antA*::*lacZ* transcriptional fusion remained inducible by anthranilate in strain ACN194, in which the chromosomal copy of ORF3 was disrupted. In ACN194, the fully induced LacZ levels were 70% of those in ACN107, indicating that ORF3 is not required for *antA* expression. Thus, specific roles for ORF1, ORF2, and ORF3 in anthranilate degradation were not detected.

Localization of the *ant* genes on the ADP1 chromosome. To map the *ant* genes by previously described methods (16), a *Not*I recognition sequence was introduced into the 3′ end of *antC* by using pBAC112 to replace the wild-type allele and generate ACN80 (Table 1). Following the *Not*I digestion of genomic DNA and electrophoretic separation by transverse alternating-field electrophoresis, the sizes of the six wild-type and seven ACN80 DNA fragments were compared. In ACN80, the wild-type 1,090-kbp fragment was replaced by two fragments, not present in the wild type, whose combined sizes were equal to 1,090 kbp. A labeled probe made from DNA upstream of *antC* between the *Cla*I sites in *antA* and *antB* (Fig. 2) hybridized to the wild-type 1,090-kbp *Not*I fragment and to an 810-kbp *Not*I fragment of ACN80. In addition, this probe hybridized to a 490-kbp *Not*I fragment of a *trpD* mutant, ACN30, in which there is a *Not*I recognition site at map position 3290 (hybridization data not shown). Collectively, these data located the *antC* gene at map position 3500 and indicated its transcriptional direction to be clockwise, as depicted in Fig. 6.

Substitution of BenC for AntC. Despite the ΩS insertion in *antC*, strain ACN80 was able to grow with anthranilate as the sole carbon source. A second *antC* disruption strain, ACN86 (Fig. 2; Table 1), was constructed and was also able to grow at the expense of anthranilate. When *antC* was disrupted in certain strains carrying mutations in the *ben* gene region, however, the ability to grow with anthranilate as the sole carbon source was lost. Specifically, combinations of the *antC*::Ω*S5086* allele with either the *benC*::Ω*K5106* allele (ACN115), the Δ(*benB-benC5129*) allele (ACN87), or the *benM*::Ω*K5008* allele (ACN103) eliminated growth at the expense of anthranilate. The *benM* gene encodes a transcriptional activator of *benC* expression (8). It appears, therefore, that in the absence of *antC*, *benC* was required for growth on anthranilate, most

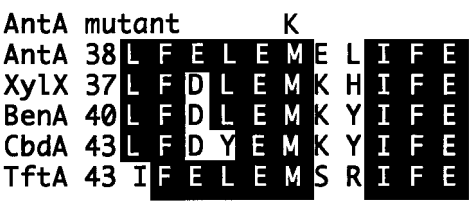

FIG. 4. Alignment of dioxygenase protein sequences in the N-terminal regions of the α subunits. A substitution of K for M in AntA causes a temperature-sensitive mutant enzyme that is dysfunctional at high temperatures. Numbers indicate the amino acid position of the adjacent residue. Residues identical to those of AntA are shown in white on a black background.

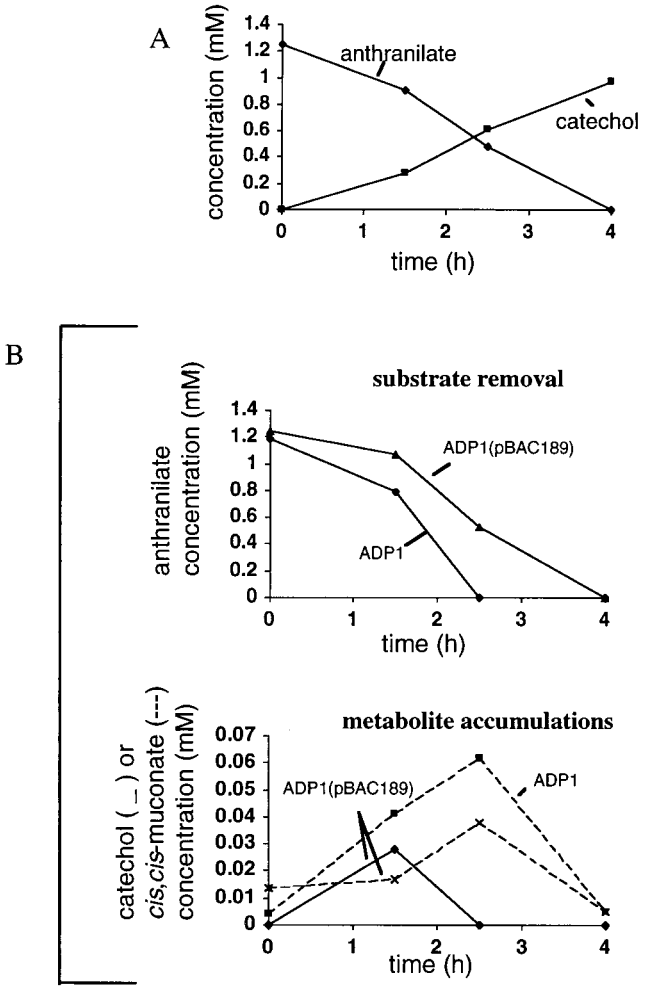

FIG. 5. Compounds in culture supernatant fractions. (A) Anthranilate was converted to catechol by *E. coli* BL21(DE3)(pBAC190) with the ADP1 *antABC* genes in *trans*. (B) During anthranilate consumption (top) by *Acinetobacter* strain ADP1 or by ADP1(pBAC189), with the *antABC* genes in *trans*, catechol and/or *cis,cis*-muconate accumulated (bottom). Prior to anthranilate addition at time zero, the growth substrate for ADP1 was anthranilate, whereas ADP1(pBAC189) was grown with both anthranilate and succinate. Concentrations were determined by HPLC methods.

likely because the BenC reductase can substitute for AntC in anthranilate oxidation.

DISCUSSION

The isolation and analysis of the *antABC* genes establish that anthranilate dioxygenase is evolutionarily related to class IB dihydroxylating enzyme systems. Dihydroxylating enzymes have been classified according to the number and types of proteins in the multicomponent complex (4, 6). Class I enzymes are comprised of a terminal oxygenase and a flavin-containing NADH-dependent reductase. In class IB enzymes the flavin cofactor is flavin adenine dinucleotide, and the reductase contains a plant-type [2Fe-2S] cluster and a presumed mononuclear iron center. The terminal dioxygenase contains a Rieske-type [2Fe-2S] cluster. In anthranilate dioxygenase, there are two subunits in the terminal oxygenase, the larger of which, the α subunit, is presumed to contain both the Rieske-type iron-sulfur and mononuclear iron centers.

In addition to the anthranilate dioxygenase-dependent route for anthranilate catabolism (21), there are at least two other evolutionarily distinct aerobic pathways for degrading this compound. Some eukaryotic microbes use a flavoprotein monooxygenase, anthranilate hydroxylase, to convert anthranilate to 2,3-dihydroxybenzoate (36). In addition, a novel pathway for the aerobic degradation of anthranilate by a denitrifying *Pseudomonas* strain, which has some characteristics of both aerobic and anaerobic degradative routes, has been described (1, 2).

Anthranilate dioxygenase and the homologous *cbd*-encoded enzyme produce catechol from their substrates, whereas the *xyl*- and *ben*-encoded dioxygenases yield nonaromatic *cis*-diols that are converted to catechol in subsequent NAD^+-dependent dehydrogenase-mediated steps. The direct formation of catechol most likely results from the spontaneous decarboxylation and loss of the *ortho* substituent when these steps are energetically favorable. No *cis*-diol is detected during CbdABC-mediated 2-halobenzoate degradation (13, 18), and, similarly, none was detected during anthranilate catabolism (Fig. 5). The inference that the chemical nature of the substrate determines whether a catechol or a *cis*-diol will form is consistent with observations by Nakatsu et al. (30) that the requirement for the CbaC dehydrogenase, following hydroxylation by the CbaAB chlorobenzoate dioxygenase, depends on the substrate. In this example, a *cis*-diol is formed when the substrate is 3-chlorobenzoate, but when the substrate is 3,4-dichlorobenzoate, elimination of HCl occurs spontaneously, obviating the need for a dehydrogenase (30).

Comparisons of anthranilate and benzoate dioxygenases. The presence of *benC* allowed strains lacking *antC* to degrade anthranilate, suggesting that the BenC reductase was able to transfer electrons from NADH to the AntAB terminal oxygenase component. Amino acids of class IB reductases that are predicted to bind flavin adenine dinucleotide, the [2Fe-2S] cluster, and those predicted to bind NADH are conserved between AntC and BenC (6, 34). Amino acids in these reductases that define substrate specificity, like those involved in protein-protein contacts with the terminal oxygenases, have yet

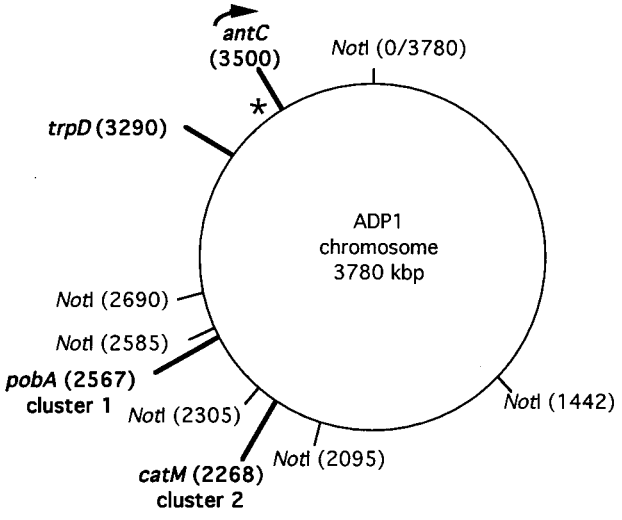

FIG. 6. Genome map of ADP1. The positions of genes are shown relative to the six wild-type *Not*I recognition sites in the chromosome. The chromosomal ΩS insertion of ACN80 introduced a *Not*I site at map position 3500, localizing the position of *antC* as shown. The asterisk marks the position of the hybridization probe indicating the direction of transcription as shown. Clusters 1 and 2 mark the relative positions of large supraoperonic regions containing numerous genes for aromatic compound degradation; only one gene of each cluster is indicated.

to be determined. Reductases, including BenC, can donate electrons from NADH to artificial electron acceptors, demonstrating that the cognate oxygenase is not required for electron transfer. Moreover, electron transfer from several reductase components to a terminal oxygenase other than the authentic partner has previously been inferred (6, 10).

The ability of BenC to substitute for AntC requires the *ben* operon to be expressed in the presence of anthranilate. Although expression of this operon is inducible (8), low levels of constitutive gene expression may allow some BenC to facilitate the formation of catechol which can then be converted to *cis,cis*-muconate. Both of these metabolites are known inducers of BenM-activated *ben* gene transcription (8). Consistent with this scenario, *benM* disruption prevented *benC* from substituting for *antC*. Since the *benAB* genes are cotranscribed with *benC* (8), the inability of *benA* to substitute for a defective *antA* gene cannot be attributable to insufficient gene expression. Collectively, the results indicate that the substrate specificity of these dioxygenases is determined by the terminal oxygenase component.

Although the substrate specificity of the *Acinetobacter* benzoate dioxygenase has not been studied, that from *Pseudomonas arvilla* C-1 can hydroxylate anthranilate with 25% activity relative to benzoate as the substrate (48). Whether the substrate specificity is determined by the α or β subunit, or both, remains to be investigated. An early study of toluate dioxygenase, XylXY, implicated the smaller β subunit in substrate specificity (20). Recent studies of 2-nitrotoluene 2,3-dioxygenase, however, showed that the C-terminal region of the α subunit defines this enzyme's specificity (35).

As expected, amino acids in the α subunits of the dioxygenases that are predicted to coordinate iron-sulfur clusters, or those that may bind the mononuclear nonheme iron, are highly conserved and are present in AntA (6, 34). The *antA* mutation causing anthranilate dioxygenase to be dysfunctional at 39°C, but not 25°C, occurs in the N-terminal protein region, 12 residues from a conserved histidine likely to participate in binding the Rieske [2Fe-2S] cluster (34). The mutation was predicted to replace a conserved methionine with a lysine (Fig. 4), thereby substituting a positively charged residue for one that is hydrophobic. The significance of this substitution and its possible effect on protein folding at high temperature remain to be determined.

Expression and chromosomal organization of the *antABC* genes. The clustered *antABC* genes may be cotranscribed, as are their *ben* counterparts (8). The coding regions of *antA* and *antB* are separated by only 2 nucleotides, and those of *antB* and *antC* are separated by 11 nucleotides. Studies of a chromosomal *antA*::*lacZ* transcriptional fusion, described above, indicated that *antA* expression is inducible by anthranilate itself and that the approximately 300-nucleotide region upstream of the *antA* translational start signal is probably sufficient for transcriptional control. Comparison of this region with that upstream of *benA* did not reveal any obvious regulatory signals. Studies of regulatory mutants suggested that neither of the LysR-type activators known to control benzoate and catechol degradation, BenM and CatM, controls *ant* gene expression (7).

Anthranilate-to-catechol conversion appears to be tightly regulated, since plasmid pBAC189, carrying the *antABC* genes, does not complement strains with the *antA5024* allele. The plasmid-borne *antABC* genes enable *E. coli* to convert anthranilate to catechol (Fig. 5), and, therefore, the lack of complementation in ACN84 and ACN26 may reflect toxic metabolite imbalances during anthranilate degradation by strains with the *antABC* genes in *trans*. A regulatory problem is suggested, since pBAC189 suppresses the ability of ADP1 to use anthranilate as the sole carbon source. The presence of succinate together with anthranilate allows ADP1(pBAC189) to grow, but an unusually high level of catechol accumulates from anthranilate. Succinate may allow growth of ADP1(pBAC189) by repressing *ant* gene expression and thereby limiting the levels to which catechol accumulates. Although previous studies indicate that the accumulation of catechol, per se, is not toxic at a concentration of 1 to 3 mM (14), such high levels could allow *cis,cis*-muconate to reach deleterious levels. Feedback inhibition of anthranilate dioxygenase by catechol in *Acinetobacter* strains might also play a role in controlling metabolic flow.

The *antABC* genes were not close to two supraoperonic gene clusters involved in aromatic compound degradation. The *ben* and *cat* genes, involved in benzoate and catechol degradation, respectively, are grouped together in a region greater than 20 kbp in length. This region, cluster 2 (Fig. 6), is separated from the *antABC* genes by approximately one-third of the ADP1 chromosome (16). In contrast, the *Pseudomonas aeruginosa ant* loci map to a region between the *ben* and *cat* genes (50, 51). Although the *P. aeruginosa ant* loci are involved in the catabolism of anthranilate, individual gene functions have not been assigned, nor have these genes been characterized (38). In ADP1, *antABC* provide an unusual example of genes associated with the β-ketoadipate pathway that do not map either to the *ben-cat* cluster or to a region, also greater than 20 kbp, that includes genes of the protocatechuate branch of the pathway (cluster 1 in Fig. 6) (16). The clustering of many *Acinetobacter* and *Pseudomonas* catabolic genes raises questions not only about the evolutionary origin of these regions but also about their relationships with catabolic plasmids (19, 50, 51). Future studies are needed to determine whether additional genes involved in aromatic compound degradation are in the vicinity of the *antABC* genes of ADP1.

ACKNOWLEDGMENTS

We gratefully acknowledge D. Matthew Eby for contributions to plasmid construction, enzyme assays, and HPLC monitoring studies. We thank Kim Gallagher, for genomic mapping and mutation localization, and Ketan Patel, for the initial mutant isolation studies. We also thank George Gaines, Don Kurtz, and Barny Whitman for helpful suggestions.

This research was supported by National Science Foundation grant MCB-9507393.

REFERENCES

1. **Altenschmidt, U., and G. Fuchs.** 1992. Purification and characterization of 2-aminobenzoate-CoA ligase, localization of the gene on a 8-kbp plasmid, and cloning and sequencing of the gene from a denitrifying *Pseudomonas* sp. Eur. J. Biochem. **205:**721–727.
2. **Altenschmidt, U., M. Bokranz, and G. Fuchs.** 1992. Nucleotide sequence of the plasmid carrying the gene for the flavoprotein 2-aminobenzoate-CoA monooxygenase/reductase in a denitrifying *Pseudomonas* sp. Eur. J. Biochem. **207:**715–722.
3. **Altman, E.** Unpublished observation.
4. **Bertini, I., M. A. Cremonini, S. Ferretti, I. Lozzi, C. Luchinat, and M. S. Viezzoli.** 1996. Arene hydroxylases: metalloenzymes catalysing dioxygenation of aromatic compounds. Coordination Chem. Rev. **151:**145–160.
5. **Bradford, M. M.** 1976. A rapid and sensitive method for the quantitation of microgram quantities of protein utilizing the principle of protein-dye binding. Anal. Biochem. **72:**248–254.
6. **Butler, C. S., and J. R. Mason.** 1997. Structure-function analysis of the bacterial aromatic ring-hydroxylating dioxygenases. Adv. Microb. Physiol. **38:**47–84.
7. **Collier, L. S., B. M. Bundy, and E. L. Neidle.** Unpublished observation.
8. **Collier, L. S., G. L. Gaines III, and E. L. Neidle.** 1998. Regulation of benzoate degradation in *Acinetobacter* sp. strain ADP1 by BenM, a LysR-type transcriptional activator. J. Bacteriol. **180:**2493–2501.
9. **Collier, L. S., N. N. Nichols, and E. L. Neidle.** 1997. *benK* encodes a hydrophobic permease-like protein involved in benzoate degradation by *Acinetobacter* sp. strain ADP1. J. Bacteriol. **179:**5943–5946.
10. **Danganan, C. E., R. W. Ye, D. L. Daubaras, L. Xun, and A. M. Chakrabarty.**

1994. Nucleotide sequence and functional analysis of the genes encoding 2,4,5-trichlorophenoxyacetic acid oxygenase in *Pseudomonas cepacia* AC1100. Appl. Environ. Microbiol. **60:**4100–4106.
11. **Devereaux, J., P. Haeberli, and O. Smithies.** 1984. A comprehensive set of sequence analysis programs for the VAX. Nucleic Acids Res. **12:**387–395.
11a. **Dijkshoorn, L.** Personal communication.
12. **Eraso, J. M., and S. Kaplan.** 1994. *prrA*, a putative response regulator involved in oxygen regulation of photosynthetic gene expression in *Rhodobacter sphaeroides*. J. Bacteriol. **176:**32–43.
13. **Fetzner, S., R. Muller, and F. Lingens.** 1992. Purification and some properties of 2-halobenzoate 1,2-dioxygenase, a two-component enzyme system from *Pseudomonas cepacia* 2CBS. J. Bacteriol. **174:**279–290.
14. **Gaines, G. L., III, L. Smith, and E. L. Neidle.** 1996. Novel nuclear magnetic resonance spectroscopy methods demonstrate preferential carbon source utilization by *Acinetobacter calcoaceticus*. J. Bacteriol. **178:**6833–6841.
15. **Gallegos, M. T., C. Michan, and J. L. Ramos.** 1993. The XylS/AraC family of regulators. Nucleic Acids Res. **21:**807–810.
16. **Gralton, E. M., A. L. Campbell, and E. L. Neidle.** 1997. Directed introduction of DNA cleavage sites to produce a high-resolution genetic and physical map of the *Acinetobacter* sp. strain ADP1 (BD413UE) chromosome. Microbiology **143:**1345–1357.
17. **Gregg-Jolly, L. A., and L. N. Ornston.** 1990. Recovery of DNA from the *Acinetobacter calcoaceticus* chromosome by gap repair. J. Bacteriol. **172:** 6169–6172.
18. **Haak, B., S. Fetzner, and F. Lingens.** 1995. Cloning, nucleotide sequence, and expression of the plasmid-encoded genes for the two-component 2-halobenzoate 1,2-dioxygenase from *Pseudomonas cepacia* 2CBS. J. Bacteriol. **177:**667–675.
19. **Harayama, S., M. Rekik, A. Bairoch, E. L. Neidle, and L. N. Ornston.** 1991. Potential DNA slippage structures acquired during evolutionary divergence of *Acinetobacter calcoaceticus* chromosomal *benABC* and *Pseudomonas putida* TOL pWW0 plasmid *xylXYZ*, genes encoding benzoate dioxygenases. J. Bacteriol. **173:**7540–7548.
20. **Harayama, S., M. Rekik, and K. N. Timmis.** 1986. Genetic analysis of a relaxed substrate specificity aromatic ring dioxygenase, toluate 1,2-dioxygenase, encoded by TOL plasmid pWW0 of *Pseudomonas putida*. Mol. Gen. Genet. **202:**226–234.
21. **Harwood, C. S., and R. E. Parales.** 1996. The β-ketoadipate pathway and the biology of self-identity. Annu. Rev. Microbiol. **50:**553–590.
22. **Hayaishi, O., and R. Y. Stanier.** 1951. The bacterial oxidation of tryptophan. III. Enzymatic activity of cell-free extracts from bacteria employing the aromatic pathway. J. Bacteriol. **62:**691–709.
23. **Juni, E.** 1972. Interspecies transformation of *Acinetobacter*: genetic evidence for a ubiquitous genus. J. Bacteriol. **112:**917–931.
24. **Juni, E., and A. Janik.** 1969. Transformation of *Acinetobacter calcoaceticus* (*Bacterium anitratum*). J. Bacteriol. **98:**281–288.
25. **Keen, T., S. Tamaki, D. Kobayashi, and D. Trollinger.** 1988. Improved broad-host-range plasmids for DNA cloning in Gram-negative bacteria. Gene **70:**191–197.
26. **Kobayashi, S., and O. Hayaishi.** 1970. Anthranilic acid conversion to catechol. Methods Enzymol. **17A:**505–510.
27. **Kobayashi, S., S. Kuno, N. Itada, and O. Hayaishi.** 1964. O^{18} studies on anthranilate hydroxylase—a novel mechanism of double hydroxylation. Biochem. Biophys. Res. Commun. **16:**556–561.
28. **Kokotek, W., and W. Lotz.** 1989. Construction of a *lacZ*-kanamycin-resistance cassette, useful for site-directed mutagenesis and as a promoter probe. Gene **84:**467–471.
29. **Miller, J. H.** 1972. Experiments in molecular genetics. Cold Spring Harbor Laboratory, Cold Spring Harbor, N.Y.
30. **Nakatsu, C. H., M. Providenti, and R. C. Wyndham.** 1997. The *cis*-diol dehydrogenase *cbaC* gene of Tn5271 is required for growth on 3-chlorobenzoate but not 3,4-dichlorobenzoate. Gene **196:**209–218.
31. **Neidle, E. L., and L. N. Ornston.** 1986. Cloning and expression of *Acinetobacter calcoaceticus* catechol 1,2-dioxygenase structural gene *catA* in *Escherichia coli*. J. Bacteriol. **168:**815–820.
32. **Neidle, E. L., C. Hartnett, and L. N. Ornston.** 1989. Characterization of *Acinetobacter calcoaceticus catM*, a repressor gene homologous in sequence to transcriptional activator genes. J. Bacteriol. **171:**5410–5421.
33. **Neidle, E., C. Hartnett, L. N. Ornston, A. Bairoch, M. Rekik, and S. Harayama.** 1992. *Cis*-diol dehydrogenases encoded by the TOL pWW0 plasmid *xylL* gene and the *Acinetobacter calcoaceticus* chromosomal *benD* gene are members of the short-chain alcohol dehydrogenase superfamily. Eur. J. Biochem. **204:**113–120.
34. **Neidle, E. L., C. Hartnett, L. N. Ornston, A. Bairoch, M. Rekik, and S. Harayama.** 1991. Nucleotide sequences of the *Acinetobacter calcoaceticus benABC* genes for benzoate 1,2-dioxygenase reveal evolutionary relationships among multicomponent oxygenases. J. Bacteriol. **173:**5385–5395.
35. **Parales, J. V., R. E. Parales, S. M. Resnick, and D. T. Gibson.** 1998. Enzyme specificity of 2-nitrotoluene 2,3-dioxygenase from *Pseudomonas* sp. strain JS42 is determined by the C-terminal region of the a subunit of the oxygenase component. J. Bacteriol. **180:**1194–1199.
36. **Powlowski, J. B., S. Dagley, V. Massey, and D. P. Ballou.** 1987. Properties of anthranilate hydroxylase (deaminating), a flavoprotein from *Trichosporon cutaneum*. J. Biol. Chem. **262:**69–74.
37. **Prentki, P., and H. M. Krisch.** 1984. In vitro insertional mutagenesis with a selectable DNA fragment. Gene **29:**303–313.
37a. **Rosche, B., B. Tshisuaka, B. Hauer, F. Lingens, and S. Fetzner.** 1997. 2-Oxo-1,2-dihydroquinoline 8-monooxygenase: phylogenetic relationship to other multicomponent nonheme iron oxygenases. J. Bacteriol. **179:**3549–3554.
38. **Rosenberg, S. L., and G. D. Hegeman.** 1971. Genetics of the mandelate pathway in *Pseudomonas aeruginosa*. J. Bacteriol. **108:**1270–1276.
39. **Sambrook, J., E. F. Fritsch, and T. Maniatis.** 1989. Molecular cloning: a laboratory manual, 2nd ed. Cold Spring Harbor Laboratory Press, Cold Spring Harbor, N.Y.
40. **Schirmer, F., S. Ehrt, and W. Hillen.** 1997. Expression, inducer spectrum, domain structure, and function of MopR, the regulator of phenol degradation in *Acinetobacter calcoaceticus* NCIB8250. J. Bacteriol. **179:**1329–1336.
41. **Schoenlein, P. V., B. B. Roa, and M. E. Winkler.** 1989. Divergent transcription of *pdxB* and homology between the *pdxB* and *serA* gene products in *Escherichia coli* K-12. J. Bacteriol. **171:**6084–6092.
42. **Shanley, M. S., E. L. Neidle, R. E. Parales, and L. N. Ornston.** 1986. Cloning and expression of *Acinetobacter calcoaceticus catBCDE* genes in *Pseudomonas putida* and *Escherichia coli*. J. Bacteriol. **165:**557–563.
43. **Simon, R., U. Priefer, and A. Puhler.** 1983. A broad host range mobilization system for in vivo genetic engineering: transposon mutagenesis in gram-negative bacteria. Bio/Technology **1:**37–45.
44. **Studier, F. W., A. H. Rosenburg, J. J. Dunn, and J. W. Dubendorff.** 1990. Use of T7 RNA polymerase to direct expression of cloned genes. Methods Enzymol. **185:**60–89.
45. **Tabor, S., and C. C. Richardson.** 1985. A bacteriophage T7 RNA polymerase/promoter system for controlled exclusive expression of specific genes. Proc. Natl. Acad. Sci. USA **82:**1074–1078.
46. **Taniuchi, H., M. Hatanaka, S. Kuno, O. Hayaishi, M. Nakajima, and N. Kurihara.** 1964. Enzymatic formation of catechol from anthranilic acid. J. Biol. Chem. **239:**2204–2211.
47. **Williams, P. A., and L. Shaw.** 1997. *mucK*, a gene in *Acinetobacter calcoaceticus* ADP1 (BD413), encodes the ability to grow on exogenous *cis,cis*-muconate as the sole carbon source. J. Bacteriol. **179:**5935–5942.
48. **Yamaguchi, M., and H. Fujisawa.** 1980. Purification and characterization of an oxygenase component in benzoate 1,2-dioxygenase system from *Pseudomonas arvilla* C-1. J. Biol. Chem. **255:**5058–5063.
49. **Yanisch-Perron, C., J. Vieira, and J. Messing.** 1985. Improved M13 phage cloning vectors and host strains: nucleotide sequences of the M13mp18 and pUC19 vectors. Gene **33:**103–119.
50. **Zhang, C., and B. W. Holloway.** 1992. Physical and genetic mapping of the *catA* region of *Pseudomonas aeruginosa*. J. Gen. Microbiol. **138:**1097–1107.
51. **Zhang, C., M. Huang, and B. W. Holloway.** 1993. Mapping of *ben* genes of *Pseudomonas aeruginosa*. FEMS Microbiol. Lett. **112:**255–260.